Rev. Adv. Mater. Sci. 43 (2015) 52-60

TOUGHENING DUE TO CRACK DEFLECTION IN CERAMIC- AND METAL-GRAPHENE NANOCOMPOSITES

I.A. Ovid'ko[1,2,3] and A.G. Sheinerman[1,2,3]

[1]Research Laboratory for Mechanics of New Nanomaterials,
Peter the Great St. Petersburg Polytechnic University, St. Petersburg 195251, Russia
[2]Department of Mathematics and Mechanics, St. Petersburg State University, St. Petersburg 198504, Russia
[3]Institute of Problems of Mechanical Engineering, Russian Academy of Sciences,
St. Petersburg 199178, Russia

Received: September 15, 2015

Abstract. A model is suggested which describes fracture toughness of ceramics and nanocrystalline metals containing graphene (nano)platelets with random orientations. Within the model, the toughening is primarily associated with two-dimensional deflection of cracks that bypass graphene nanoplatelets. Using the boundary element method, it is demonstrated that two-dimensional crack deflection can increase fracture toughness by up to 90 percent. It is shown that the optimum graphene concentration that corresponds to maximum toughening is determined by the aspect ratio of graphene nanoplatelets. The results of the model explain the results of the experiments demonstrating strong toughening of ceramics containing graphene nanoplatelets. The situation where graphene nanoplatelets have the same orientation is also briefly discussed.

1. INTRODUCTION

With its combination of a large specific surface area and excellent mechanical properties, graphene is a very promising candidate for the use as a nanofiller in various composite materials [1–14]. For example, the studies of composites containing polymer-based matrices (e.g., [2,15–22]) demonstrate that graphene inclusions can considerably enhance the mechanical properties of polymers. Also, in recent years, several research groups have fabricated metal–matrix nanocomposites reinforced by graphene inclusions [8–13,23], which exhibit very high strength and hardness. In addition, recently, graphene nanoplatelets (also referred to as graphite nanoplatelets) – inclusions containing several monolayers of graphene, with a thickness from 1 nm to several tens of nanometers – have been used to produce ceramic–graphene composites [24–37]. The characterizations of such composites demonstrated that graphene nanoplatelets lead to significant improvements of fracture toughness, flexural strength and electrical conductivity of ceramics [24–37]. In particular, it was revealed that small graphene concentrations (that is, small volume fractions of graphene inclusions) can result in significant toughening of ceramics. For instance, Walker et al. [26] reported 135% increase in fracture toughness of silicon nitride through the addition of 1.5 vol.% of multilayer graphene sheets. Walker et al. [26] attributed the observed strong toughening primarily to the formation of dense ensembles of graphene sheets that encapsulate individual grains and induce crack deflection. Ramirez et al. [36] produced silicon nitride ceramics toughened either by reduced graphene oxide sheets (multilayer graphene oxide sheets with a high ratio of carbon atoms to that of oxygen atoms) or by very thin (1 nm in thickness)

Corresponding author: I.A. Ovid'ko, e-mail: ovidko@nano.ipme.ru

graphene nanoplatelets. They reported 135% increase in fracture toughness of silicon nitride toughened by 4.3 vol.% of reduced graphene oxide and 40% increase in fracture toughness of silicon nitride toughened by 4.3 vol.% of graphene nanoplatelets. At the same time, similar studies of Al_2O_3 and Al_2O_3-based ceramics toughened by graphene nanoplatelets [28,31–34] as well as other experimental investigations of graphene–Si_3N_4 composites [27,29] have not demonstrated such strong toughening.

Besides ceramics, graphene inclusions can potentially toughen nanocrystalline metals. In such metals, lattice dislocation motion is suppressed, resulting in low toughness of nanocrystalline metals [38]. Similar to the case of ceramics, the introduction of graphene nanoplatelets in the nanocrystalline matrix should hinder crack propagation and can produce nanocomposites with very high strength and satisfactory toughness.

The mechanisms responsible for the toughening of ceramics and nanocrystalline metals by graphene nanoplatelets can be crack deflection, crack bridging and crack branching, and all these mechanisms have been observed in ceramic–graphene composites (e.g., [26–30, 33,34]). At the same time, the possible contribution of each mechanism to fracture toughness is not clear. Also, the scattered experimental data on fracture toughness of ceramic–graphene composites [26–37] do not allow one to reveal the effects of the geometry of graphene nanoplatelets and structure of ceramics on the fracture toughness of ceramic–graphene composites as well as to estimate the maximum possible fracture toughness that can be achieved by the insertion of graphene nanoplatelets into ceramics. To fill this gap, in the present paper, we suggest a model that describes the toughening of ceramic–graphene and graphene–nanocrystalline metal composites with a focus on the crack deflection mechanism of toughening. In the following sections, we present a model of crack growth in ceramics and nanocrystalline metals containing graphene nanoplatelets, calculate their fracture toughness and compare it with available experimental data.

2. CRACK PROPAGATION IN A BRITTLE SOLID TOUGHENED BY GRAPHENE NANOPLATELETS. MODEL

Consider a brittle solid (ceramics or nanocrystalline metal) toughened by graphene nanoplatelets (Fig. 1a). For simplicity, we examine a two-dimensional model, where graphene nanoplatelets represent elongated rectangles whose length is much larger than their thickness. We consider the situation where graphene nanoplatelets have different random orientations (Fig. 1a). Let us examine a brittle crack that propagates in a composite (containing graphene nanoplatelets) under a uniaxial tensile stress (Figs. 1b and 1c). We postulate that the crack cannot penetrate graphene nanoplatelets or initiate formation of new cracks on the other side of nanoplatelets. Also, we will not consider such toughening mechanisms as crack bridging and pull-out of graphene nanoplatelets or crack branching and focus on toughening associated with crack deflection. Thus, within the model, when a crack propagating through a matrix grain (Fig. 1b) or along a grain boundary (Fig. 1c) meets a graphene nanoplatelet, it changes its direction and advances along the matrix–graphene interface. Next, when the crack has propagated along the matrix–graphene interface, it again changes its direction and grows either through a matrix grain or along a grain boundary. (The latter situation is possible only if the

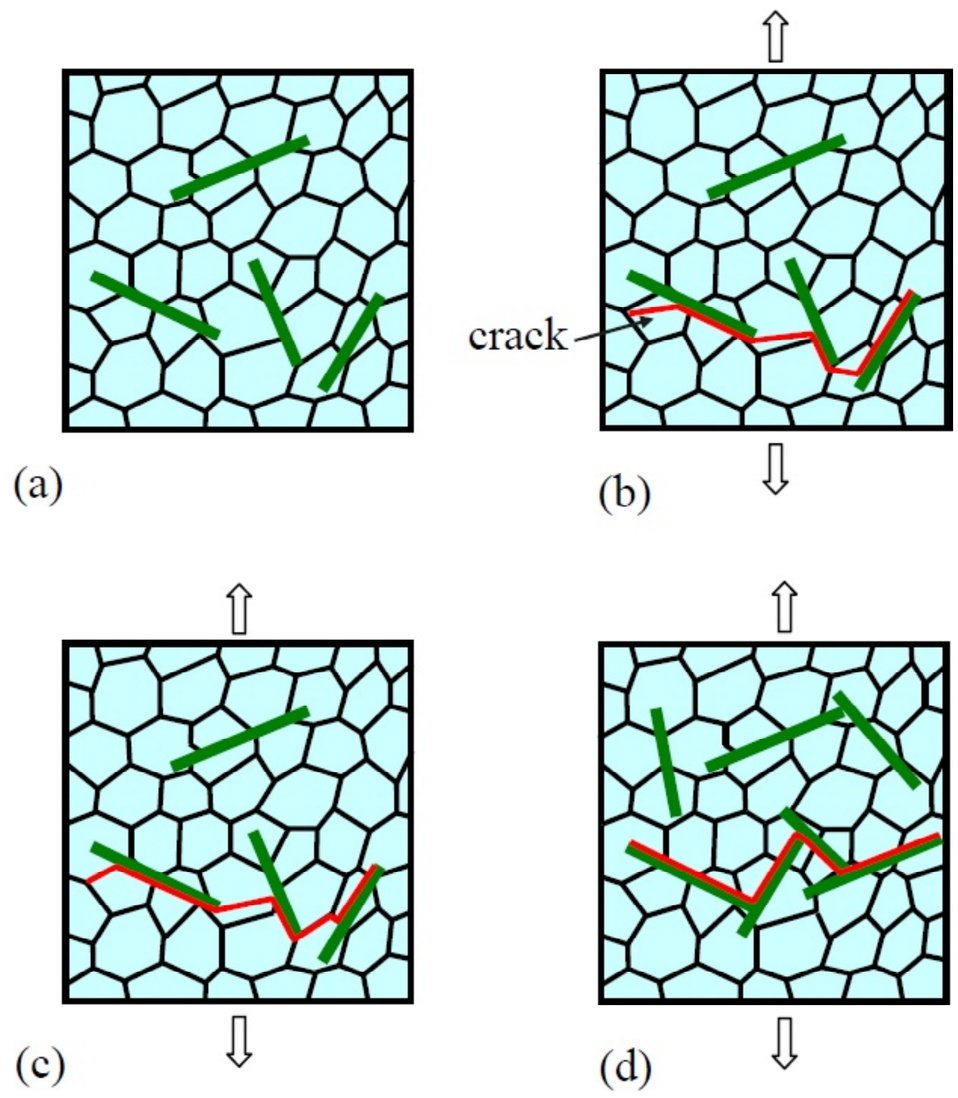

Fig. 1. Crack propagation in a composite consisting of a polycrystalline or nanocrystalline matrix and graphene nanoplatelets (two-dimensional view). (a) Composite without a crack. (b) Crack in the composite propagates through matrix grains and along matrix–graphene interfaces. (c) Crack in the composite propagates along matrix grain boundaries, through matrix grains and along matrix–graphene interfaces. (d) Crack in the composite propagates only along matrix–graphene interfaces.

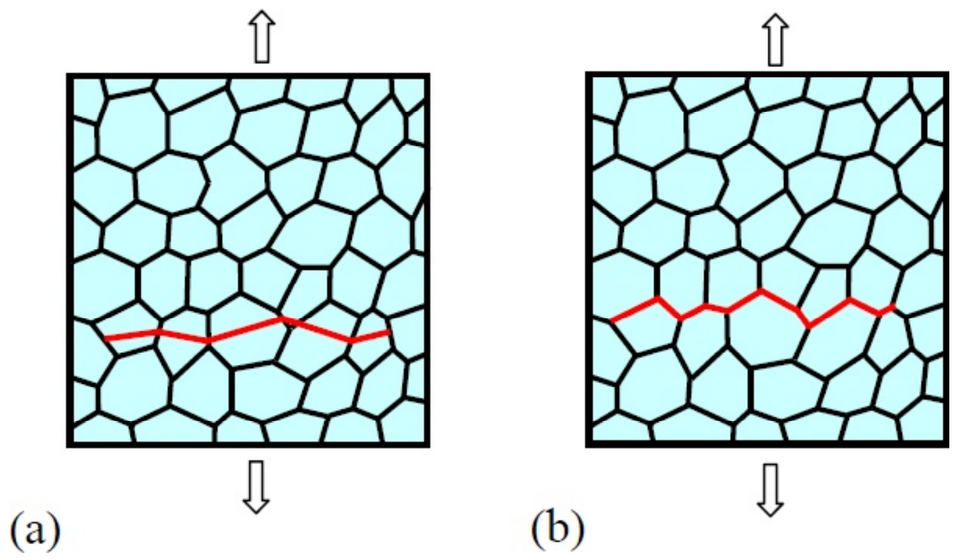

Fig. 2. Crack propagation in a polycrystalline or nanocrystalline matrix. (a) Crack propagates through grains along favorable crystal planes that vary from one grain to another. (b) Crack propagates along grain boundaries.

graphene nanoplatelet terminates at a grain boundary.) After that, the crack meets a new graphene nanoplatelet, and the process repeats (Figs. 1b and 1c). Thus, on a large scale, the crack direction is normal to the direction of the applied load, while graphene nanoplatelets induce local fluctuations of the direction of crack propagation, which increase fracture toughness.

To compare the fracture toughness of brittle solids toughened by graphene nanoplatelets with that of similar solids without graphene inclusions, one should take into consideration that even in pure ceramics or nanocrystalline metals, the cracks are not necessarily ideally straight. Intragrain cracks can deviate from the plane normal to the direction of the applied load and advance along favorable planes with small surface energies, thereby propagating in a zigzag fashion (Fig. 2a). Grain boundary cracks propagate along grain boundaries that also make large enough angles with the normal to the crack plane (Fig. 2b).

Also, for the calculation of the fracture toughness of brittle solids toughened by graphene nanoplatelets, one should account for the fact that intragrain crystallographic planes, grain boundaries and matrix–graphene interfaces have different resistance to crack propagation. (The propagation of a crack along a grain boundary or a matrix–graphene interface is expected to be easier than that along a favorable crystallographic plane making the same angle with the normal to the direction of the applied load.) Thus, in the calculation of the fracture toughness it is reasonable to consider the most difficult region for crack propagation, that is, its propagation inside a matrix grain. Besides, one should notice that even if cracks in pure ceramics or nanocrystalline metals tend to propagate along grain boundaries (Fig. 2b), in similar solids toughened by graphene nanoplatelets, cracks can advance not only along grain boundaries and matrix–graphene interfaces but also inside matrix grains (Fig. 1c). (This is because graphene nanoplatelets are typically larger than grain boundaries and, in general, terminate inside grains.) In the latter case the change

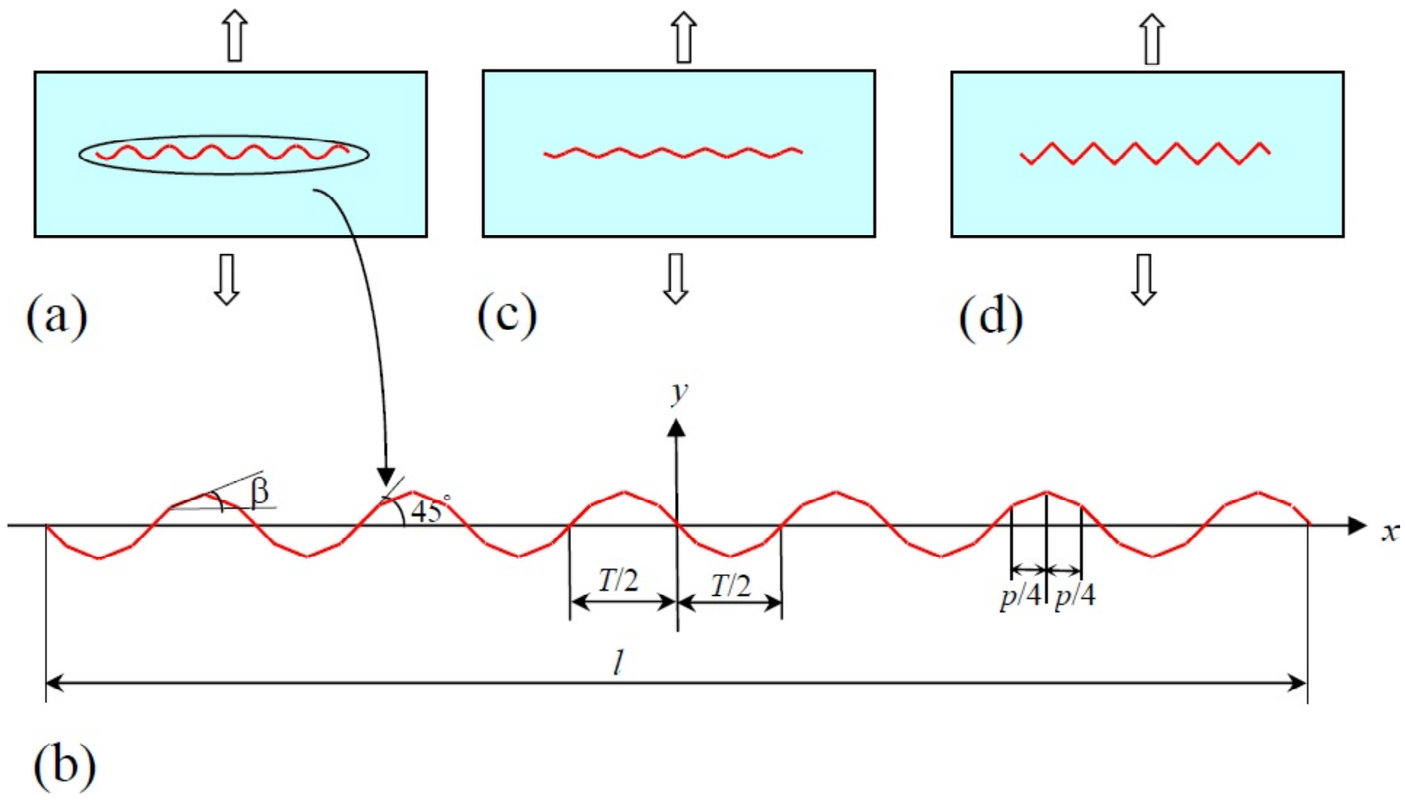

Fig. 3. Geometry of model cracks in the composites containing graphene inclusions and pure ceramics or metals under uniaxial tensile loading. (a) Model crack in a composite containing graphene inclusions. (b) Geometry of the crack shown in (a). The crack propagates along matrix–graphene interfaces (inclined by ±45° with respect to the *x*-axis) and favorable crystallographic directions in the matrix (inclined by the angle ±β with respect to the *x*-axis). (c) Model intragrain crack in a polycrystalline or nanocrystalline solid. The crack consists of the fragments inclined by the angle ±β with respect to the *x*-axis. (d) Model grain boundary crack in a polycrystalline or nanocrystalline solid. The crack consists of the fragments inclined by the angle ±30° with respect to the *x*-axis.

of the fracture mode (from grain boundary fracture to mixed grain boundary and transgranular fracture) also leads to the toughening of the composites containing graphene inclusions. At the same time, if the concentration of graphene nanoplatelets exceeds a critical value, the latter can form a cluster (Fig. 1d). In this situation, fracture toughness is determined by the small resistance of matrix–graphene interfaces to crack propagation and is expected to be smaller than fracture toughness of similar solids containing isolated graphene nanoplatelets.

Now let us calculate the fracture toughness of the composites containing graphene nanoplatelets. In general, the fracture toughness of such composites depends on the concentration of graphene nanoplatelets, their dimensions, their locations relative to each other and their orientation with respect to the direction of the applied stress. The variations in the orientation of graphene nanoplatelets can result in essential variations in the toughness characterizing propagation of different cracks. Therefore, as a first approximation, to estimate average fracture toughness, we consider an idealized periodic structure where all graphene nanoplatelets have the same dimensions and make the angles of ±45° with the normal to the direction of the applied load (Figs. 3a and 3b). We also assume that intragrain and grain boundary crack fragments make angles $\pm\beta$ with the normal to the direction of the applied load, the distances passed by the crack along all matrix–graphene interfaces are the same, and the distances passed by the crack between neighboring graphene nanoplatelets are also the same (Fig. 3b). Within the model, the crack is periodic with a period T, and its length l is much larger than T (Fig. 3b). The parameter p determines the total distance $p/\cos\beta$ that the crack passes between graphene nanoplatelets within each period. In the limiting case of $p = T$, where graphene nanoplatelets are absent, the crack transforms to a model periodic intragrain (Fig. 3c) or grain boundary (Fig. 3d) crack in a pure ceramics or nanocrystalline metal.

3. CALCULATION OF FRACTURE TOUGHNESS OF THE COMPOSITES CONTAINING GRAPHENE NANOPLATELETS

Let us consider the effect of crack deflection on the fracture toughness of a composite containing graphene nanoplatelets. To do so, as a first approximation, we will model the composite as an isotropic solid with the shear modulus G and Poisson's ratio ν. We will also use the standard crack growth criterion [39] based on the balance between the driving force related to a decrease in the strain energy and the hampering force related to formation of new free surfaces during crack growth. In the examined case of the plane strain state, this criterion is given by [39]

$$\frac{1-\nu}{2G}\left(K_I^2 + K_{II}^2\right) = 2\gamma_e, \qquad (1)$$

where K_I and K_{II} are the stress intensity factors for normal (to crack line) and shear loading, respectively, and γ_e is the effective specific surface energy. Here we put $\gamma_e = \gamma$ (where γ is the specific surface energy) if the crack advances inside a matrix grain, and $\gamma_e = \gamma_c$ (where γ_c is the specific cohesive energy of the matrix–graphene interface) for the crack that grows along a matrix –graphene interface.

Within the macroscopic mechanical description, the effect of crack deflection on crack growth can be accounted for through the introduction of the critical stress intensity factor K_{IC}. In this case, the crack is considered as that propagating under the action of the tensile load perpendicular to the crack growth direction, while crack deflection simply changes the value of K_{IC} compared to the case of straight crack propagation. In these circumstances, the critical condition for the crack growth can be represented as (see, e.g., [40]): $K_I^s = K_{IC}$, where K_I^s is the stress intensity factor created by a uniaxial tensile load near the tip of a straight crack.

Now let us introduce the parameters α_1 and α_2, such that $K_I = \alpha_1 K_I^s$ and $K_{II} = \alpha_2 K_I^s$. Substituting the latter relations and the equality $K_I^s = K_{IC}$ to formula (1), we obtain $K_{IC} = \sqrt{4G\gamma_e / \left[(1-\nu)\left(\alpha_1^2 + \alpha_2^2\right)\right]}$. For convenience, we introduce the quantity $K_{IC}^s = \sqrt{4G\gamma/(1-\nu)}$ describing fracture toughness associated with propagation of a straight intragrain crack. Then we have

$$\frac{K_{IC}}{K_{IC}^s} = \sqrt{\frac{\gamma_e/\gamma}{\alpha_1^2 + \alpha_2^2}}. \qquad (2)$$

It is important to note that formula (2) is valid for the two-dimensional cracks where all parts of the crack front simultaneously propagate either inside the matrix or along the matrix-graphene interface. In this case, fracture toughness is determined by the region where crack propagation is most difficult inside the matrix. At the same time, in the case of real three-dimensional cracks, some parts of the crack front propagate inside the matrix, whereas the other parts of the crack front propagate along matrix–graphene interfaces with a very small cohe-

sive strength and, as a result, a small effective surface energy γ_e. Therefore, if the crack front is straight, the surface energy γ in formula (2) should be replaced by an appropriate average of the values of the effective surface energy γ_e over the crack front, including a small value γ_c for the parts propagating along the matrix–graphene interface. As a result, in this case, the fracture toughness K_{IC} will be lower than that for the examined two-dimensional cracks.

In reality, of course, the crack front may not be straight, in which case the "easy" parts of the crack front (propagating along the matrix–graphene interfaces) will advance further towards the "difficult" positions (characterized by propagation inside the matrix). In doing so, however, they increase the stress intensity factor at the parts of the crack front that have already been in the "difficult" positions, helping them to propagate further. Thus, our two-dimensional model leads to some overestimation of the effective fracture toughness associated with crack deflection compared to the real three-dimensional case.

Using the boundary element method (e.g., [41]), we have numerically calculated the parameters α_1 and α_2 for $l/T = 10$, various values of the ratio p/T, and $\beta = 30°$ and 15°. The case $p/T = 1$ corresponds to the fracture toughness of a pure ceramics or nanocrystalline metal (Figs. 3b and 3c). If cracks in a pure ceramics or nanocrystalline metal propagate in a transgranular mode (Fig. 3c), we have: $\gamma_e = \gamma$. If cracks in a ceramics or nanocrystalline metal propagate along grain boundaries (Fig. 3d), we have: $\gamma_e = \gamma - \gamma_b/2$, where γ_b is the specific grain boundary energy. In the latter case (Fig. 3d), we also put $\beta = 30°$, which represents the average value of the angle between the grain boundary plane and the macroscopic crack growth direction in the model case of regular hexagonal grains. Thus, using the computed values of α_1 and α_2 for $p/T = 1$ at $\beta = 30°$ and 15° and setting $\gamma_b = 0.4\,\gamma$, we obtain the fracture toughness K_{IC}^0 for model cracks in a pure ceramics or nanocrystalline metal (see Figs. 3c and 3d) to be as follows: for intragrain cracks (Fig. 3c), $K_{IC}^0/K_{IC}^s = 1.247$ and 1.748 at $\beta = 15°$ and 30°, respectively, and for grain boundary cracks (Fig. 3d), $K_{IC}^0/K_{IC}^s = 1.563$.

Now let us calculate the fracture toughness K_{IC} of the composites containing graphene nanoplatelets as a function of the volume concentration c of graphene nanoplatelets. Let each graphene nanoplatelet represent a rectangular parallelepiped with a thickness h and a square base with the side length p_0. Let $\Delta = T/2$ be the average distance between the centers of neighboring graphene nanoplatelets. Then the volume V of the composite per one graphene nanoplatelet can be estimated as $V \approx \Delta^3$, and the volume concentration c of graphene can be written as $c = p_0^2 h/\Delta^3$. We assume that the average distance that the crack passes along a graphene sheet (having the length p_0) is $p_0/2$. Then for the situation shown in Fig. 3b, we have: $(p_0/2)\cos(\pi/4) = (T - p)/2$, which yields: $p_0 = (T - p)\sqrt{2}$. The latter relation along with the relations $c = p_0^2 h/\Delta^3$ and $\Delta = T/2$ gives:

$$c = \frac{16\sqrt{2}h}{p_0}\left(1 - \frac{p}{T}\right)^3. \qquad (3)$$

At $p/T = 0$, the graphene concentration c reaches the critical value $c_{cr} = 16\sqrt{2}\,h/p_0$ at which graphene nanoplatelets form a cluster.

Formula (3) demonstrates that increasing the length p_0 of graphene nanoplatelets and/or decreasing their thickness h reduces c at a given p/T. Since the value of p/T determines the value of fracture toughness K_{IC}, this means that the concentration c of graphene nanoplatelets needed to obtain a specified value of K_{IC} is the smaller, the longer and thinner the nanoplatelets are. At the same time, the thickness of graphene nanoplatelets should not be too small (below one to several nm). The reason is that a very thin graphene nanoplatelet cannot serve as a barrier for the generation of a crack (at the opposite side of the graphene nanoplatelet) in the stress field of a pre-existent large crack that approaches the nanoplatelet.

Using the calculated values of K_{IC} for various values of p/T and formula (3), we have calculated the dependences of the normalized fracture toughness K_{IC}/K_{IC}^0 on the graphene volume concentration c, for various values of the angle β. One should note that the dimensions h and p_0 of graphene nanoplatelets can vary in a wide range. For example, Walker et al. [26] fabricated composites containing graphene nanoplatelets with $h \approx 1$ nm and p_0 around 100 to 500 nm. Porwal et al. [34] produced composites containing nanoplatelets with $h \approx 1$ nm and $p_0 \approx 1.5$ μm. Liu et al. [32] obtained composites containing graphene nanoplatelelts with $h = 8$ to 10 nm and p_0 around 1 to 5 μm. Therefore, for definiteness, we put: $h/p_0 = 0.002$. The calculated dependences of K_{IC}/K_{IC}^0 on the graphene volume concentration c are plotted in Fig. 4 for the case of $c < c_{cr}$. Fig. 4 demonstrates that graphene nanoplatelets increase the fracture toughness of ceramics and nanocrystalline metals. The maximum fracture toughness of a composite containing graphene

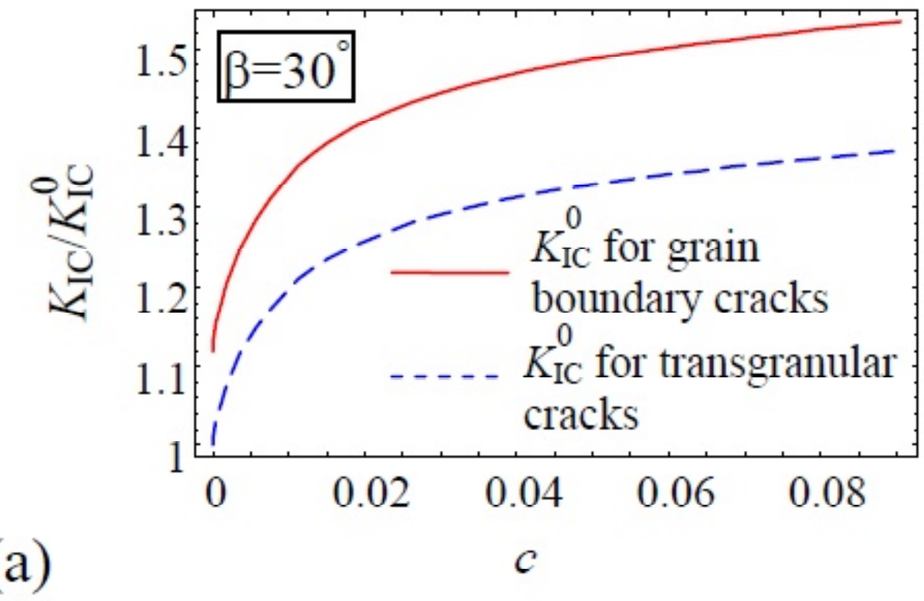

Fig. 4. The ratios of fracture toughness K_{IC} of the brittle solid toughened by graphene nanoplatelets to the fracture toughness K_{IC}^0 of a similar solid without graphene nanoplatelets as functions of the graphene concentration c, for various values of the angle β characterizing the oscillations of the crack direction in a brittle solid without graphene nanoplatelets.

nanoplatelets corresponds to the case where the concentration c approaches the critical one ($c \to c_{cr}$), when c is close to c_{cr} but still smaller than c_{cr}, so that graphene nanoplatelets do not form a cluster. Fig. 4 also shows that if cracks in the matrix tend to propagate along grain boundaries, the introduction of an optimum (for toughening) concentration of graphene nanoplatelets can increase fracture toughness approximately by 50%. At the same time, if cracks in the matrix tend to propagate through grains, the introduction of an optimum concentration of graphene nanoplatelets can increase fracture toughness by 50–90%, depending on the value of the angle β. Fig. 4 also demonstrates that at small graphene concentrations c, K_{IC} very quickly grows with c, while at larger c, an increase in graphene concentration leads only to a slight increase in fracture toughness K_{IC}. In particular, for the values of graphene nanoplatelet dimensions ($h/p_0 = 0.002$) used to plot Fig. 4, significant toughening is observed already at $c = 0.01$ or even smaller, that is, at the graphene concentration of 1 vol.% or less. At $c = c_{cr}$ (the right ends of the dependences in Fig. 4), fracture toughness is expected to abruptly drop due to the formation of a cluster of graphene nanoplatelets, which are expected to serve as the paths of easy crack propagation.

Formula (3) and Fig. 4 also demonstrate that the optimum (for toughening) values of graphene concentration (corresponding to the case $c \to c_{cr}$) strongly depends on the aspect ratio h/p_0 of graphene platelets: the smaller platelet thickness h and larger platelet length and width p_0, the smaller concentration of graphene platelet is needed to provide the maximum fracture toughness of the composite containing graphene nanoplatelets.

4. FRACTURE TOUGHNESS OF CERAMIC–GRAPHENE COMPOSITES: COMPARISON WITH EXPERIMENTS

Now let us compare the calculated values of fracture toughness of the composites containing graphene nanoplatelets with available experimental data on ceramic–graphene composites. It should be noted that the experimental values of fracture toughness of such composites vary in a wide range. In particular, as is mentioned above, using Vickers indentation testing, Walker et al. [26] observed 135% increase in fracture toughness of Si_3N_4 by the addition of 1.5 vol.% of graphene nanoplatelets. Ramirez et al. [36], using the surface crack in flexure method, reported 135% increase in fracture toughness of silicon nitride toughened by 4.3 vol.% of reduced graphene oxide. Centeno et al. [31], using the indentation-strength method, documented 50% increase in fracture toughness of Al_2O_3 through the addition of 0.22 vol.% of graphene nanoplatelets. As is seen in Fig. 4, these values of fracture toughness enhancement are much higher than the calculated fracture toughness enhancement associated with two-dimensional crack deflection in the presence of randomly oriented graphene platelelts. At the same time, the authors of works [27–29,32–34] observed significantly lower toughening associated with graphene nanoplatelets. For example, Tapaszto et al. [27] compared the mechanical properties of carbon nanotube (CNT)– and graphene–Si_3N_4 composites for 3 wt.% graphene concentration. They demonstrated an enhancement of 10–50% in the mechanical properties (fracture toughness, hardness, bending strength, Young's modulus) for graphene composites compared to CNT compos-

ites with the same concentration, although the overall properties for both composites decreased compared to pure Si_3N_4. Kvetkova et al. [29], using Vickers indentation testing, reported 45% increase in fracture toughness for 1 wt.% graphene–silicon nitride composites consolidated using high isiostatic pressing. Wang et al. [28], using the single edge notched beam method, reported 53% increase in fracture toughness of graphene–alumina composites for the graphene concentration of 2 vol.%. Bódis et al. [37], using the Vickers indentation method, revealed 45% increase in fracture toughness for 1 wt.% graphene–silicon nitride composites consolidated through spark plasma sintering. Liu et al [32], using the single edge notched beam method, revealed fracture toughness increase of Al_2O_3 by 27% at 0.22 vol.% of graphene nanoplatelets. Liu et al. [33] and Porwal et al. [34], using the single edge notched beam method and Vickers indentation testing, documented fracture toughness enhancement by 40% at 0.8% of graphene nanoplatelets added to Al_2O_3–Zr composite [33] or pure Al_2O_3 [34]. Besides, Ramirez et al. [36], using the surface crack in flexure method, reported 40% increase in fracture toughness of silicon nitride toughened by 4.3 vol.% of graphene nanoplatelets. The toughening observed in experiments [28, 29, 32–34, 37] is in good agreement with our calculations (see Fig. 4b).

Note that experiments [29,32–34,36,37] showed that fracture toughness of ceramic–graphene composites first increases and then decreases with increasing graphene concentration. At the same time, the experimental values of the critical concentration (above which fracture toughness starts to drop) are often [29,32–34, 37] very small, being well below 2 vol.%. Since such concentrations are sometimes smaller than the concentration c_{cr} required to form large graphene clusters, a decrease in fracture toughness can also be associated with the increasing porosity [32–34,37], in particular, with the formation of pores around graphene nanoplatelets. At the same time, Fig. 4 demonstrates that suppressing porosity would allow fabrication of ceramic–graphene composites with higher graphene concentration that would provide stronger toughening.

Concerning the difference in toughening documented in experiments [26,31] and that documented in experiments [28,29,32–34] and obtained in our calculations, one should note that toughening depends on the orientation of graphene nanoplatelets, which can be highly anisotropic if the ceramic–graphene composites are consolidated using the spark plasma sintering method. This is associated with uniaxial pressure applied during sintering of ceramic–graphene nanoplatelets, which drives graphene nanoplatelets to lie in the plane perpendicular to the pressure direction [34]. This alignment of graphene can also enhance the toughness of the materials in the direction perpendicular to graphene sheets but does not increase the toughness in the planes parallel to graphene sheets. In particular, Centeno et al. [31] revealed that fracture toughness increases by 50% for cracks parallel to the direction of sintering and does not increase at all for crack normal to this direction. One can also assume that very high toughening observed in experiment [26] can, at least, partly, be associated with the preferable orientation of graphene sheets and is valid for unfavorable crack orientations (that is, for the cracks whose macroscopic growth direction is close to the normal to graphene sheets) but not necessarily for cracks parallel to them.

Thus, graphene nanoplatelets can increase fracture toughness for cracks growing in any direction only if such nanoplatelets have random orientations. Our calculations demonstrate that in the latter case, two-dimensional crack deflection associated with the presence of graphene nanoplatelets can increase fracture toughness of ceramics by up to 40-90%, depending on graphene concentration and preferable fracture mode of ceramics (intergranular or transgranular). At the same time, other toughening mechanisms – crack bridging and graphene sheet pull-out or crack branching – observed [28,29,33,34,36] in ceramic–graphene composites also contribute to the fracture toughness of these composite structures. The effect of these mechanisms on fracture toughness manifests itself mainly at long (above 100 μm) crack lengths [26], providing higher fracture toughness for long cracks. At the same time, although Fig. 4 demonstrates that crack deflection can significantly increase the fracture toughness of ceramic–graphene composites, our model does not allow one to estimate the percentage of the contribution of this toughening mechanism to overall toughening. Further research is needed to clarify this issue.

In addition, note that undulations of graphene sheets can also be a mechanism responsible for high fracture toughness of ceramic–graphene composites. Actually, such undulation were observed in experiments [26, 36] (for silicon nitride toughened by reduced graphene oxide), where very high toughening was observed. Also, Ref. [36] reported strong undulations of reduced graphene oxide sheets, which toughened silicon nitride by up to 135%, and

much flatter geometry of graphene nanoplatelets, which toughened the same ceramics only by up to 40%. All this testifies that along with crack deflection, bridging and sheet pull-out and, the bending of graphene sheets can also contribute to the toughening of ceramic–graphene composites.

5. CONCLUSIONS

Thus, in this paper we have suggested a model describing toughening of ceramics and nanocrystalline metals containing graphene nanoplatelets with random orientations. Within the model, the toughening is associated with two-dimensional deflection of cracks that bypass graphene nanoplatelets. We have considered model periodic cracks that approximately describe real cracks that bypass graphene nanoplatelets during growth. Using the boundary element method, we have calculated the critical stress intensity factor for deflecting mode I cracks, which describes fracture toughness of the composites containing graphene inclusions. As a reference structure, we have examined pure ceramics or nanocrystalline metals containing either transgranular or grain boundary cracks. The results demonstrated that the addition of randomly oriented graphene nanoplatelets to a ceramics or nanocrystalline metal can increase fracture toughness by up to 50%, if the cracks in the pure ceramics or nanocrystalline metal grow along grain boundaries, and by up to 90%, if such cracks tend to be transgranular. These values correlate well with the results of experiments [23,24,27–29,32] on ceramic–graphene composites. Thus, our calculations confirm that crack deflection is an important toughening mechanism that can lead to significant enhancement of the fracture toughness of ceramic–graphene composites. We have also demonstrated that the optimum (for toughening) graphene concentration strongly depends on the aspect ratio h/p_0 of graphene nanoplatelets and decreases with a decrease in the nanoplatelet thickness h and/or an increase in the nanoplatelet length p_0. At the same time, if graphene nanoplatelets have the same orientation, these can considerably increase fracture toughness for the cracks normal to the graphene nanoplatelets but hardly provide essential toughening for the cracks growing parallel to these nanoplatelets. The effect of the graphene nanoplatelet orientation on the fracture toughness of ceramic–graphene composites provides the opportunity for fabrication of composites with various mechanical properties by tuning the geometry of graphene nanoplatelets.

ACKNOWLEDGEMENTS

This work was supported by the Russian Science Foundation (Research Project 14-29-00199).

REFERENCES

[1] T. Kuilla, S. Bhadha, D. Yao, N.H. Kim, S. Bose and J.H. Lee // *Prog. Polymer. Sci.* **35** (2010) 1350.
[2] I.A. Ovid'ko // *Rev. Adv. Mater. Sci.* **34** (2013)19.
[3] A. Nieto, D. Lahiri and A.Agarwal // *Mater. Sci. Eng.* A **582** (2013) 338.
[4] X. Shi, B. Peng, N.M. Pugno and H. Gao // *Appl Phys Lett* **100** (2012) 191913.
[5] N.M. Pugno and T. Abdalrahman // *Nanoscience and Nanotechnology Letters* **4** (2012) 1064.
[6] B. Liu, C.D. Reddy, J. Jiang, J.A. Baimova, S.V. Dmitriev, A.A. Nazarov and K. Zhou // *Phys. Rev.* B **101** (2012) 211909.
[7] J.A. Baimova, S.V. Dmitriev and K. Zhou // *Phys. Status Solidi* B **249** (2012) 1393.
[8] J. Wang, Z. Li, G. Fan, H. Pan, Z. Chen and D. Zhang // *Scr. Mater*. **66** (2012) 594.
[9] Y. Kim, J. Lee, M.S. Yeom, J.W. Shin, H. Kim, Y. Cui, J.W. Kysar, J. Hone, Y. Jung, S. Jeon and S.M. Yan // *Nature Commun.* **4** (2013) 2114.
[10] J. Hwang, T. Yoon, S.Y. Jin, J. Lee, T.-S. Kim, S.H. Hong and S. Jeon // *Adv. Mater.* **25** (2013) 6724.
[11] D. Kuang, L. Xu, L. Liu, W. Hu and Y. Wu // *Appl. Surf. Sci.* **273** (2013) 484.
[12] C.L.P. Pavithra, B.V. Sarada, K.V. Rajulapoti, T.N. Rao and D. Sundararajan // *Sci. Rep.* **4** (2014) 4049.
[13] I.A. Ovid'ko // *Rev. Adv. Mater. Sci.* **38** (2014) 190.
[14] I.A. Ovid'ko and A.G. Sheinerman // *J. Phys. D* **47** (2014) 495302.
[15] S. Stankovich, D.A. Dikin, G.H.B. Dommett, K.M. Kohlhaas, E.J. Zimney, E.A. Stach, R.D. Piner, S.B.T. Nguyen and R.S. Ruoff // *Nature* **442** (2006) 282.
[16] T. Ramanathan, A.A. Abdala, S. Stankovich, D.A. Dikin, M. Herrera-Alonso, R.D. Piner, D.H. Adamson, H.C. Schniepp, X. Chen and R.S. Ruoff // *Nat. Nanotechnol.* **3** (2008) 327.
[17] M.A. Rafiee, J. Rafiee, I. Srivastava, Z. Wang, H. Song, Z.Z. Yu and N. Koratkar // *Small* **6** (2010) 179.
[18] J.R. Potts, D.R. Dreyer, C.W. Bielawski and R.S. Ruoff // *Polymer* **52** (2011) 5.

[19] E.Jomehzadeh, A.R. Saidi and N.M. Pugno // *Physica* E **44** (2012) 1973.
[20] T.K. Das and S. Prusty // *Polymer-Plastics Technology and Engineering* **52** (2013) 319.
[21] J. Du and H.-M. Cheng // *Macromol. Chem. Phys.* **213** (2013) 1060.
[22] Y.J. Noh, H.I. Joh, J. Yu, S.H. Hwang, S. Lee, C.H. Lee, S.Y. Kim and J.R. Youn // *Sci. Rep.* **5** (2015) 9141.
[23] K. Chu and C. Jia // *Phys Status Solidi* A **211** (2014) 184.
[24] T. He, J. Li, L. Wang, J. Zhu and W. Jiang // *Mater. Trans.* **50** (2009) 749.
[25] Y. Fan, L. Wang, J. Li, S. Sun, F. Chen, L. Chen and W. Jiang // *Carbon* **48** (2010) 1743.
[26] L.S. Walker, V.R. Marroto, M.A. Rafiee, N. Koratkar and E.L. Corral // *ACS Nano* **5** (2011) 3182.
[27] O. Tapaszto, L. Tapaszto, M. Marko, F. Kern, R. Gadow and C. Balazsi // *Chem. Phys. Lett.* **511** (2011) 340.
[28] K. Wang, Y. Wang, Z. Fan, J. Yan and T. Wei // *Mater. Res. Bull.* **46** (2011) 315.
[29] L. Kvetkova, A. Duszova, P. Hvizdos, J. Dusza, P. Kun and C. Balazsi // *Scr. Mater*. **66** (2012) 793.
[30] H. Porwal, S. Gresso and M.J. Reece // *Adv. Appl. Ceram*. **112** (2013) 443.
[31] A. Centeno, V.G. Rocha, B. Alonso, A. Fernandez, C.F. Gutierres-Gonzalez, R. Torrecillas and A. Zurutuza // *J. Eur. Ceram. Soc.* **33** (2013) 3201.
[32] J. Lui, H. Yan and K. Jiang // *Ceramics Intern.* **39** (2013) 6215.
[33] H. Porwal, P. Tatarko, S. Grasso, J. Khaliq, I. Dlouhy and M.J. Reece // *Carbon* **64** (2013) 359.
[34] J. Lui, H. Yan, M.J. Reece and K. Jiang // *J. Eur. Cer. Soc.* **32** (2012) 4185.
[35] Y. Fan, M. Estili, G. Igarashi, W. Jiang and A. Kawasaki // *J. Eur. Ceram. Soc.* **34** (2014) 443.
[36] C. Ramirez, P. Miranzo, M. Belmonte, M.I. Osendi, P. Poza, S.M. Vega-Diaz and M. Terronez // *J. Eur. Ceram. Soc.* **34** (2014) 161.
[37] E. Bódis, O. Tapasztó, Z. Károly, P. Fazekas, S. Klébert, A.M. Keszler, K. Balázsi and J. Szépvölgyi // *Open Chem.* **13** (2015) 484.
[38] C.C. Koch, I.A. Ovid'ko, S. Seal and S. Veprek, *Structural Nanocrystalline Materials: Fundamentals and Applications* (Cambridge University Press, Cambridge, 2007).
[39] R.G. Irwin // *J. Appl. Mech.* **24** (1957) 361.
[40] *Fracture Mechanics and Strength of Materials*, ed. by V.V.Panasyuk (Naukova Dumka, Kiev, 1988), vol. 2, In Russian.
[41] A. Becker, *The Boundary Element Method in Engineering* (McGraw-Hill, New York, 1992).